Biochimica et Biophysica Acta 1842 (2014) 623–634

Contents lists available at ScienceDirect

Biochimica et Biophysica Acta

journal homepage: www.elsevier.com/locate/bbadis

Wiskott–Aldrich Syndrome causing mutation, Pro373Ser restricts conformational changes essential for WASP activity in T-cells

Neeraj Jain [1], Bhawana George [1], Thirumaran Thanabalu *

School of Biological Sciences, Nanyang Technological University, 60 Nanyang Drive, Singapore 637551, Republic of Singapore

ARTICLE INFO

Article history:
Received 2 July 2013
Received in revised form 4 January 2014
Accepted 8 January 2014
Available online 15 January 2014

Keywords:
Cell migration
T-cell activation
Immunodeficiency
IL-2 expression
Actin cytoskeleton

ABSTRACT

Wiskott–Aldrich Syndrome (WAS) is caused by mutations in Wiskott-Aldrich Syndrome Protein (WASP) and majority of the mutations are found in the WASP Homology $_1$ (WH_1) domain which mediates interaction with WIP (WASP Interacting Protein), a WASP chaperone. Two point mutations together in the proline rich region (PRR) domain of WASP (S339Y/P373S) have been reported to cause WAS however the molecular defect has not been characterized. Expression of these mutants separately ($WASP_R^{S339Y}$, $WASP_R^{P373S}$) or together ($WASP_R^{SP/YS}$) did not rescue the chemotaxis defect or membrane projection defect of $Jurkat^{WKD}$ T-cells (WASP knockdown). This is not due to the inability of WASP-PRR mutants to form functional WASP–WIP complex in growth rescue experiments in *las17Δ* yeast strain. Expression of $WASP_R^{S339Y}$ but not $WASP_R^{P373S}$ or $WASP_R^{SP/YS}$ rescued the IL-2 expression defect of $Jurkat^{WKD}$ T-cells, suggesting that Pro373Ser mutation alone is sufficient to inhibit WASP functions in T-cell activation. The diffused localization of WASP-PRR mutants in activated Jurkat T-cells suggests that Ser339 and Pro373 are critical for WASP localization. WASP-PRR mutations either together or individually did not abolish interaction of WASP with sixteen WASP binding proteins including Hck, however they caused reduction in Hck mediated tyrosine phosphorylation of WASP which is critical for WASP activity. The auto-inhibitory conformation of $WASP^{P373S}$ mutant was not relieved by the binding of Toca-1 or Nck1. Thus, our results suggest that Pro373Ser mutation reduces Tyr291 phosphorylation and prevents conformational changes required for WASP activity in chemotaxis and T-cell activation. Thus Pro3373Ser is probably responsible for all the defects associated with WAS in the patients.

© 2014 Elsevier B.V. All rights reserved.

1. Introduction

Wiskott–Aldrich Syndrome (WAS) is an X-linked immunodeficiency disorder characterized by eczema, bloody diarrhea and recurrent infections [1,2]. The gene mutated in the syndrome was identified by positional mapping and subsequently cloned [3]. Identification of the gene led to the discovery that mutation in this gene also gives rise to other two related disorders, X-linked thrombocytopenia (XLT) [4] and X-linked neutropenia (XLN) [5]. WASP is expressed predominantly in cells of hematopoietic lineage [6]. T-cells from WAS patients are characterized by fewer microvilli like projections, defects in chemotaxis and failure to proliferate upon activation [7–9]. WASP knockout mouse is viable with defects in T-cell activation [10,11]. All these are manifestations of a defective cytoskeleton [12].

WASP gene encodes a proline rich adaptor protein WASP, with several functional domains; WASP homology 1 (WH1) domain at the N-terminal followed by a basic region (BR), a GTPase binding domain (GBD), a proline rich sequence and a Verprolin homology, Cofilin homology, and Acidic region (VCA) domain at the C-terminus [13]. The N-terminal WH1 domain (aa 1–138) mediates interaction with the verprolin family of proteins (WIP, WIRE and CR16) [14] while the C-terminal VCA domain activates the actin nucleation activity of Arp2/3 complex [13,15].

A large number of missense point mutations in WASP have been identified from patients with different degrees of severity such as Wiskott–Aldrich Syndrome (WAS), X-linked thrombocytopenia (XLT) and X-linked neutropenia (XLN) [16,17]. However the links between mutations and disease have not been characterized. Majority of the missense mutations in WASP are located in the WH1 domain of WASP [17], the region important for interaction with WASP interacting protein (WIP) [6]. Some of the missense mutations in the WH1 domain of WASP have been shown to affect WASP–WIP interaction [18,19]. WIP is a chaperone for WASP and loss of interaction with WIP leads to the proteolytic cleavage of WASP and WASP deficiency [20]. Out of 52 WASP missense mutations reported [17], 12 missense mutations are present outside the WH1 domain and 5 mutations causing classic WAS in humans are located in the proline rich region (PRR) (S339Y/P373S), the WASPbase [21] and the VCA domain (P459S, K476E and D485N) of WASP [17].

WASP has been shown to adopt a closed inactive conformation due to intra-molecular interaction between the acidic region of the VCA domain and the basic region adjacent to the GBD [22]. We have previously used bimolecular complementation assay to show that the closed conformation of WASP is stabilized by WIP [23]. This closed conformation

* Corresponding author. Tel.: +65 63162832; fax: +65 6791 3856.
E-mail address: thirumaran@ntu.edu.sg (T. Thanabalu).
[1] Tel.: +65 63162832; fax: +65 6791 3856.

0925-4439/$ – see front matter © 2014 Elsevier B.V. All rights reserved.
http://dx.doi.org/10.1016/j.bbadis.2014.01.006

can be relieved by Toca-1 or Nck1 which binds to the PRR of WASP [23]. Proline rich region of WASP is crucial for localization of WASP to the immunological synapse [24] and has been shown to interact with the SH3 domain of tyrosine kinases and adaptor proteins [17,25]. However the molecular defect caused by mutation in the proline rich region of WASP has not been identified. Characterizing the molecular defect of mutations ($WASP^{P373S}$, $WASP^{S339Y}$) at proline rich region of WASP will lead to a better understanding of the regulation of WASP by SH3 domain containing proteins.

In this study we generated a WASP knockdown Jurkat T-cell ($Jurkat^{WKD}$) and found the $Jurkat^{WKD}$ T-cells to have reduced migration velocity, defective chemotaxis, and defective upregulation of IL-2 transcription. Expression of WT WASP rescued all the defects while expression of $WASP^{P373S}$ or $WASP^{PS/SY}$ did not rescue any of the defects of the $Jurkat^{WKD}$ T-cells. Expression of $WASP^{S339Y}$ rescued the IL-2 transcription defect of $Jurkat^{WKD}$ T-cells but not the chemotaxis defect. Conformational analysis suggests that $WASP^{P373S}$ adopts a closed conformation just like the WT WASP but unlike WT WASP the closed conformation of $WASP^{P373S}$ was not relieved in the presence of Toca1 or Nck1 even though both Toca1 and Nck1 can bind to $WASP^{P373S}$.

2. Materials and methods

2.1. Yeast strains, media, cell lines, reagents and antibodies

Saccharomyces cerevisiae strain PJ69-4A was used for yeast two hybrid assay and IDY166 [26] was used for growth rescue experiment. YPUAD (yeast extract, peptone, uracil, adenine and dextrose) media was used for yeast cell culture. Jurkat (clone E6-1) (ATCC, USA) was maintained in RPMI media supplemented with 10% FBS and 1% penicillin/streptomycin while Phoenix Amphotropic packaging cell line (ATCC, USA) was maintained in DMEM with 10% FBS at 37 °C CO_2 incubator. Anti-human CD3 clone OKT3 and CD28 clone CD28.2 were purchased from eBioscience. Alexa Fluor 488 and 594 phalloidin were from Molecular Probes. G418-sulfate and SDF-1α were from PAA Laboratories and PeproTech respectively. Mouse monoclonal anti-WASP (D1), anti-Cdc42 and anti-GAPDH antibodies were from Santa Cruz and Ambion respectively. Mouse anti-phosphotyrosine clone-4G10 was purchased from Upstate Biotechnology (Lake Placid, NY, USA). Anti-His antibody was purchased from Delta Biolabs. All secondary antibodies conjugated with horseradish peroxidase were from Sigma-Aldrich (St. Louis, MO, USA).

2.2. Site-directed mutagenesis

QuickChange Site-Directed Mutagenesis kit from Stratagene (La Jolla, CA, USA) or Overlap Extension technique was used to generate the mutation of interest at specific locations in the human WASP cDNA sequence and cloned in EBV based plasmid and WASP promoter was used for the transcriptional regulation of WASP expression.

2.3. Retrovirus vector mediated RNAi

Phoenix Amphotropic cell line was used to generate retroviral particles. In brief, Amphotropic cells were transfected with 80 μg of plasmid encoding WASP specific shRNA (S1-WASP shRNA) (GCAGGGAATTCAGC TGAACAA) under the transcriptional control of U6 promoter and GFP under the CMV promoter using calcium phosphate transfection method. 48 h of post-transfection, cell supernatant was collected and used to transduce Jurkat T-cells. The transduced Jurkat T-cells stably expressing GFP were sorted using FACS Aria and further grown before analysis of endogenous WASP expression.

2.4. Stable transfection

Four silent mutations were introduced in WASP gene in the region targeted by S1-WASP shRNA (GCAAGGTATCCAACTGAACAA) thus making it resistant ($WASP_R$) to the silencing machinery. Gene transfections in Jurkat T-cells were performed using Neon transfection system (Invitrogen, CA, USA) according to manufacturer's instructions. In brief, $Jurkat^{WKD}$ T-cells were microporated (three pulses with pulse width of 10 ms at 1500 V) with 10 μg of $WASP_R$ (WT or mutants) expressing plasmid. The cells were selected with neomycin (1.5 mg/ml) (G-418) for a period of one week. Stable expression of exogenous gene was confirmed by Western blotting.

2.5. Fluorescence visualization of yeast cells

Conformational analysis of WASP or its mutants was performed using Bi-molecular Fluorescence Complementation (BiFC) assay as described previously [23]. In brief, cells grown to exponential phase were harvested at 600 ×*g* for 5 min. They were washed twice with PBS, resuspended in PBS and applied to a microscope slide. Fluorescence imaging was performed using an Olympus microscope with $CoolSNAP^{HQ}$ camera (Roper Scientific). Quantification of fluorescence intensities of 100 cells was performed using the MetaMorph software (Molecular Devices, CA, USA). The growth rescue experiment was performed as described previously [19].

2.6. Cell migration assays

Chemotaxis of migrating cells in a gradient of SDF-1α was observed using Dunn chamber (Weber Scientific International; [27]). In this assay, 2.25×10^6 Jurkat T-cells attached to the fibronectin (2 μg/ml) coated coverslip were placed onto Dunn chamber filled with complete RPMI media. The outer well media was then replaced with media containing chemokine (SDF-1α, 5 nM) and subsequently, the edges of the coverslip were sealed with a mixture of hot wax (1:1:1, paraffin wax, bees wax and vaseline). The cell migration on annular bridge between the outer and the inner well was observed and captured at 2 min interval for a period of 3 h using an inverted microscope (Olympus IX81) attached to the $CoolSNAP^{HQ}$ camera. The migration tracks were analyzed using MetaMorph software (Molecular Devices, CA, USA) and plotted. Chemotaxis was also assessed by transwell migration assay using polycarbonate membrane insert, 24 well transwell (5 μm pore size) (catalog no—3421). 2×10^5 Jurkat T-cells or $Jurkat^{WKD}$ T-cells expressing WT WASP or its mutants were added to the upper well of transwell and allowed to migrate towards the chemokine (SDF-1α, 100 ng/ml) containing RPMI media in lower well for 3 h. Cells migrated to the lower well were counted and percentages of cells migrated were plotted.

2.7. IL-2 expression assay

$Jurkat^{WKD}$ T-cells expressing WASP or mutants were stimulated with wells coated with anti-human CD3/CD28 (2 μg/ml each) for 8 h. Total RNA was isolated (Omega Bio-Tek) and converted into cDNA. Quantitative real time PCR for IL-2 gene expression was performed using thermal cycler (Applied Biosystem 7500) and SYBR Green/ROX qPCR Master Mix (Fermentas). The sense and anti-sense primers for IL-2 expression are (in 5′–3′ direction) CAAACCTCTGGAGGAAGTGCT, and AATGGTTGCTGT CTCATCAGC. Real time specific primers for human MRPL-27 (CTGGTG GCTGGAATTGACCGCTA and CAAGGGGATATCCACAGAGTACCTTG) were used for normalization.

For IL-2 cytokine secretion analysis in culture media, $Jurkat^{WKD}$ T-cells expressing WASP or mutants were resuspended in complete RPMI media at 1×10^6 cells/ml containing both mouse anti human CD3 and CD28 (2 μg/ml each) and incubated on ice for 45 min. Cells after incubation were washed and plated on 96 well plate pre-coated with anti-mouse IgG Ab (for cross-linking) (10 μg/ml). Supernatant

was collected 24 h after incubation in CO_2 incubator and examined for IL-2 by standard ELISA (PeproTech Human IL-2 kit, 900-K12).

2.8. Immunofluorescence microscopy and localization

Stable WASP or WASP mutants expressing Jurkat^{WKD} T-cells were seeded on anti-CD3/anti-CD28 (2 μg/ml each) antibody coated coverslip and incubated for 30 min in humified CO_2 incubator. Cells were fixed with 4% formaldehyde for 20 min, washed three times and stained with Alexa Flour 594 phalloidin. The mean surface area (in μm^2) and average number of membrane projections per cell of 30 cells from each population were calculated using MetaMorph software. The experiment was repeated thrice and 30 cells were evaluated in each set of the experiment. Localization study of WASP or its mutants in WT Jurkat T-cells relative to actin was performed as described [28]. In brief, WASP or its mutants (tagged with RFP) expressing cells were seeded on anti-CD3 coated (10 μg/ml) coverslip and incubated for 5 min. Coating of coverslip with antibodies was performed overnight at 4 °C. Poly-L-lysine coated coverslip was used as control. Cells after incubation were fixed with 4% formaldehyde in PBS, washed thrice with PBS and stained with Alexa Flour 488 phalloidin. Fluorescent images were captured using Olympus microscope fitted with CoolSNAP^{HQ2} camera.

2.9. T-cell–APC conjugate formation

Raji B-cells were stained with CMAC (Molecular Probes) for 30 min and then incubated with 2 μg/ml of SEE superantigen (Toxin Technologies) for 90 min at 37 °C. B- and T-cells in equal number were mixed and incubated for 30 min at 37 °C. Cells after incubation were plated on poly-L-lysine coated slides and allowed to adhere for 10 min. Cells on the slide were fixed with 3.7% formaldehyde and stained with phalloidin 488 for F-actin staining.

2.10. Statistical analysis

Data represent in all the experiments as the mean ± s.e.m. from three independent experiments. Statistical significance analysis was determined using unpaired Student's *t*-test. $P < 0.05$ was considered statistically significant.

3. Results

3.1. WASP-PRR mutants do not rescue chemotaxis defect of Jurkat^{WKD} T-cells

We have previously characterized 52 missense mutations in WASP using yeast mutant strain and found that 13 mutations out of 40 mutations in the WH1 domain affected the activity of WASP–WIP complex and none of the 12 mutations outside the WH1 domain affected the activity of the WASP–WIP complex [19]. Two mutations (S339Y/P373S) together in the proline rich region of WASP have been found in WAS patients, WASPbase [17,21]. However it is not known whether both the mutations are required to compromise the activity of WASP or what are the molecular defects caused by these mutations.

In order to analyze the effect of the mutations on the activity of WASP we generated Jurkat^{WKD} T-cells (WASP knockdown Jurkat T-cells) using WASP specific shRNA (S1-shWASP). We generated retrovirus expressing S1-shWASP under the transcriptional regulation of U6 promoter and EGFP under transcriptional regulation of CMV promoter. Jurkat T-cells were infected with the retrovirus using spinoculation and subsequently the infected cells were FACS sorted using GFP fluorescence. The FACS sorted cells were cultured and the expression of WASP was analyzed by immunoblotting with anti-WASP antibody, which showed a significant knockdown of WASP expression as determined by Western blotting and 50% knockdown as determined by qPCR (data not shown). We used $WASP_R$, resistant to the S1-shWASP to analyze the function of mutants in Jurkat^{WKD} T-cells and tagged it with RFP to distinguish between the endogenous WASP and exogenous WASP constructs. Plasmids (neomycin resistant) expressing $WASP_R$ or its mutants ($WASP_R^{S339Y}$ or $WASP_R^{P373S}$ or $WASP_R^{SP/YS}$) were microporated in Jurkat^{WKD} T-cells and selected with neomycin (G418) for one week which enabled to get more then 90% of cells expressing the exogenous gene (data not shown). The Jurkat^{WKD} T-cells expressing $WASP_R$ constructs were assayed for chemotaxis using Dunn chamber with SDF-1α as a chemo-attractant. The migration of cells in annular bridges was recorded using time-lapse microscopy over a 3 h period.

Jurkat^{WKD} T-cells migrated slower than Jurkat T-cells (data not shown) and expression of $WASP_R$ restored the migration velocity of Jurkat^{WKD} T-cells while expression of RFP (control) did not (Fig. 1B, C). The migration speed of Jurkat^{WKD} T-cells expressing $WASP_R^{S339Y}$ (1.73 μm/min), $WASP_R^{P373S}$ (1.96 μm/min) or $WASP_R^{SP/YS}$ (1.75 μm/min) was similar to Jurkat^{WKD} expressing $WASP_R$ (2.17 μm/min) while Jurkat^{WKD} T-cells expressing RFP alone (control) had a reduced velocity (0.85 μm/min) (Fig. 1B, C) suggesting that WASP mutants are able to rescue the migration speed of Jurkat^{WKD} T-cells. The overall directionality of the cell motility was analyzed by plotting circular histograms which showed that 77% of total Jurkat^{WKD} T-cells expressing $WASP_R$ moved to a position within the 40° arc facing the chemokine source whereas only 20% of the total Jurkat^{WKD} ($WASP_R^{S339Y}$) T-cells moved to within the 40° arc facing the chemokine source which was similar to the RFP (22%) expressing cells. About 30% of total Jurkat^{WKD} ($WASP_R^{P373S}$) T-cells and only 20% of total Jurkat^{WKD} ($WASP_R^{SP/YS}$) T-cells migrated to the 40° arc facing the chemokine source, indicating that mutations in either of the residues affected the ability of $WASP_R$ to rescue the chemotaxis defect of Jurkat^{WKD} T-cells (Fig. 1C, D). Chemotactic defect observed in Jurkat^{WKD} T-cells expressing $WASP_R^{S339Y}$ or $WASP_R^{P373S}$ or $WASP_R^{SP/YS}$ was not due to poor expression of respective WASP mutant proteins as Western blot analysis showed that their expression was comparable to $WASP_R$ expression (Fig. 1E).

In order to confirm the chemotactic defect of Jurkat^{WKD} T-cells expressing $WASP_R$-PRR mutants towards SDF-1α, a transwell migration assay was performed. Similar to chemotactic defects observed in Dunn chamber, the migration of Jurkat^{WKD} T-cells expressing WASP mutants was significantly impaired in transwell migration assay (40.0% of total Jurkat^{WKD} ($WASP_R^{S339Y}$) T-cells, 40.3% of total Jurkat^{WKD} ($WASP_R^{P373S}$) T-cells, 39.10% of total Jurkat^{WKD} ($WASP_R^{SP/YS}$) T-cells migrated towards SDF-1α containing media in lower well compared to 51.24% of Jurkat^{WKD} ($WASP_R$) T-cells) (Fig. 1F). Thus the data suggest that the expressions of WASP mutants ($WASP_R^{S339Y}$ or $WASP_R^{P373S}$ or $WASP_R^{SP/YS}$) do not rescue the chemotaxis defect of Jurkat^{WKD} T-cells towards chemokine SDF-1α. These results suggest a possible molecular defect giving rise to Wiskott–Aldrich Syndrome in patients with WASP$^{SP/YS}$ mutation.

3.2. WASP-PRR mutants do not rescue the membrane projection defect of Jurkat^{WKD} T-cells

WASP is required for formation of actin rich membrane projections (microvilli) as lymphocytes from WAS patients were found to have fewer microvilli, although it did not affect the expression of various surface receptors [9,29]. Similarly, WASP-deficient B-cells are defective in filopodia extension in response to bradykinin stimuli [30] suggesting that WASP plays an important role in regulating membrane projections in hematopoietic cells. Thus, to analyze the effect of the WASP-PRR mutations on WASP mediated actin cytoskeleton organization, Jurkat^{WKD} T-cells expressing $WASP_R$ or its mutants ($WASP_R^{S339Y}$, $WASP_R^{P373S}$, $WASP_R^{SP/YS}$) were stimulated for 30 min on anti-CD3/anti-CD28 coated plates. The cells were fixed, permeabilized and stained with Alexa 594 phalloidin. All the WASP-PRR mutants expressing Jurkat^{WKD} T-cells spread well on anti-CD3/anti-CD28 coated plates and formed circular actin ring (Fig. 2A, B), but formed significantly fewer membrane projections compared to $WASP_R$ expressing cells (Fig. 2C) suggesting that the inability of WASP mutants to rescue the chemotaxis defect of Jurkat^{WKD}

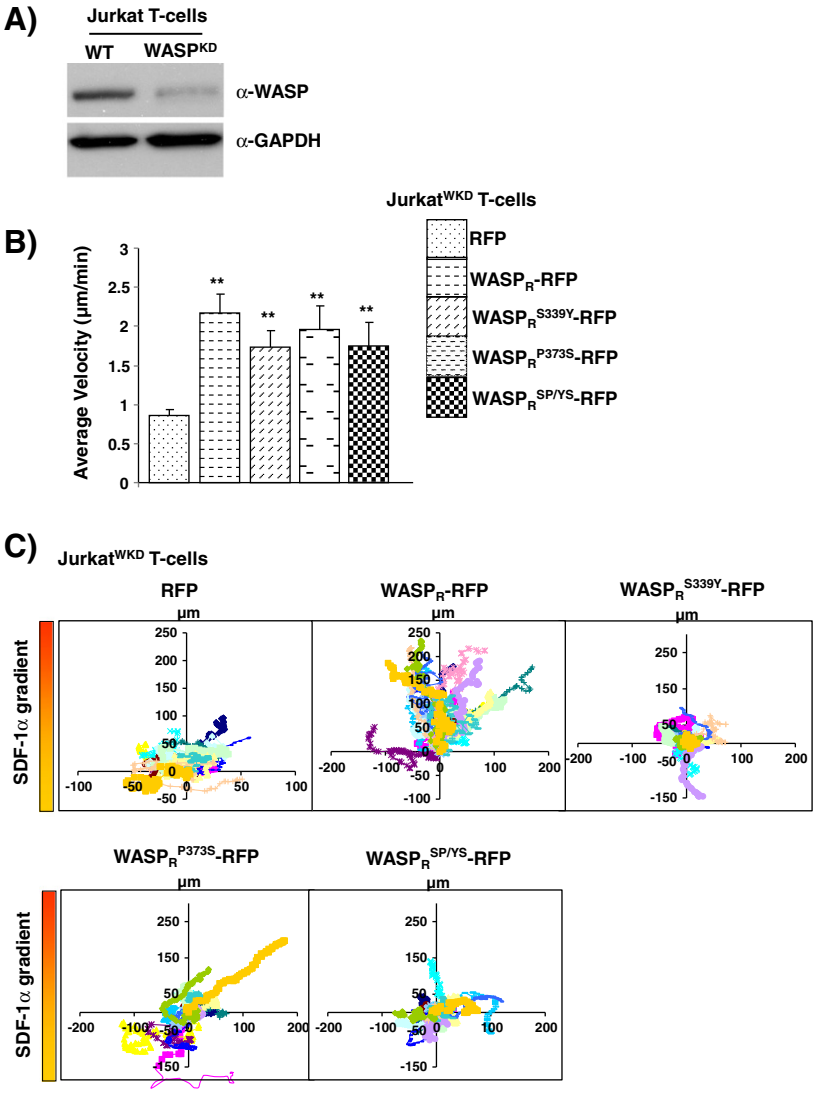
A)
Jurkat T-cells
WT
WASPKD
α-WASP
α-GAPDH
B)
JurkatWKD T-cells
Average Velocity (μm/min)
RFP
WASPR-RFP
WASPRS339Y-RFP
WASPRP373S-RFP
WASPRSP/YS-RFP
C)
JurkatWKD T-cells
SDF-1α gradient
μm

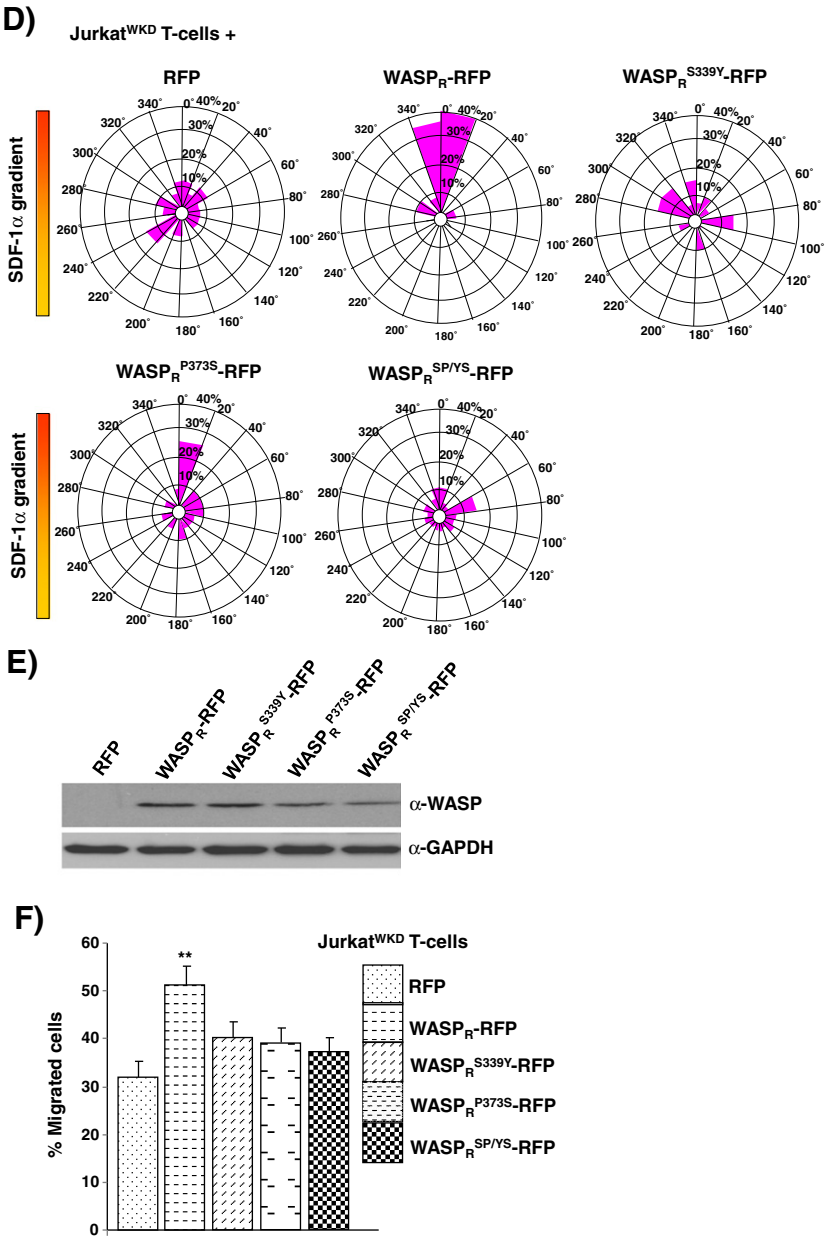
D)
JurkatWKD T-cells +
SDF-1α gradient
E)
α-WASP
α-GAPDH
F)
JurkatWKD T-cells
% Migrated cells

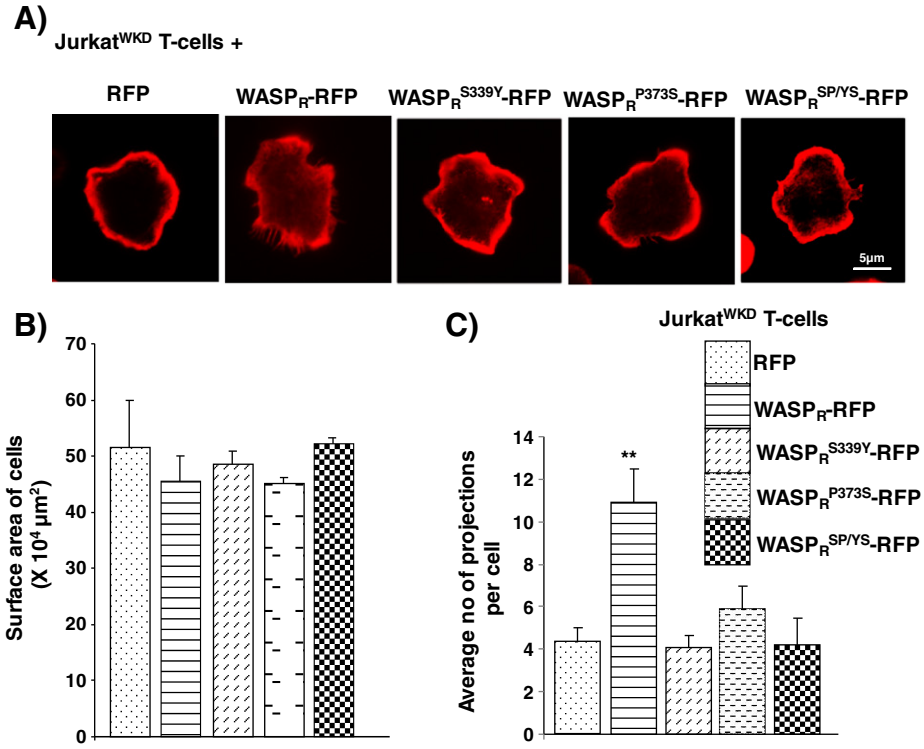

Fig. 2. Jurkat^{WKD} T-cells expressing WASP-PRR mutants were defective in actin cytoskeleton organization upon anti-CD3/anti-CD28 stimulation. A) Jurkat^{WKD} T-cells expressing (1) RFP, (2) WASP$_R$-RFP, (3) WASP$_R^{S339Y}$-RFP, (4) WASP$_R^{P373S}$-RFP, and (5) WASP$_R^{SP/YS}$-RFP were stimulated on anti-CD3/anti-CD28 (2 μg/ml each) antibody coated coverslip for 30 min, fixed with 3.7% formaldehyde and stained with Alexa 594 phalloidin. Bar = 5 μm. B) The average surface area of total 90 randomly chosen cells (30 cells in each set of three independent experiments) was quantified using MetaMorph software and plotted. C) The average number of membrane projections per cell was quantified at a total of 90 randomly chosen cells (30 cells in each set of three independent experiments). $^{**}P < 0.01$, compared to Jurkat^{WKD} T-cells expressing RFP (unpaired Student's *t*-test).

T-cells is probably due to the inability of the WASP-PRR mutants to regulate the actin cytoskeleton reorganization.

3.3. WASP-PRR mutants exhibit diffused localization at immunological synapses

The proline rich region of WASP has been shown to be important for WASP recruitment to the TCR contact sites [25]. Thus, the localization of WASP and its mutants was analyzed using Jurkat T-cells expressing WASP$_R$-RFP (WT or mutants) under the transcriptional regulation of CMV promoter. In order to study the localization pattern of WASP-PRR mutants relative to actin during TCR stimulation, Jurkat^{WT} T-cells expressing WASP$_R$-RFP or mutants (WASP$_R^{S339Y}$-RFP or WASP$_R^{P373S}$-RFP or WASP$_R^{SP/YS}$-RFP) were stimulated on anti-CD3 antibody coated plate for 5 min (at this time point, cell spreading was maximal and cells form the strongest contact with the stimulatory plane). Cells were fixed and stained with Alexa 488 phalloidin. This localization study of WASP during T-cell activation is based on a published method [28] and Jurkat^{WT} T-cells were used as Jurkat^{WKD} T-cells express GFP; therefore, it could not be used for co-localization studies. In the absence of anti-CD3 (on poly-L-lysine coated surface), Jurkat T-cells were not spread well and localization of WASP was observed throughout the T-cell cytoplasm (Fig. 3A). However, Jurkat T-cells spread well on anti-CD3 coated surface and WASP was co-localized with actin ring at the periphery of the spread cell (Fig. 3A). There was no co-localization of WASP$_R^{S339Y}$-RFP with polymerized actin ring at the periphery of the fully spread cell (Fig. 3A). Small patches of WASP$_R^{S339Y}$-RFP were observed inside the cell. Studies of cells expressing WASP$_R^{P373S}$-RFP or WASP$_R^{SP/YS}$-RFP showed that the localization of these mutants with actin ring was partially impaired (and most of these molecules were located inside the cell in a diffused pattern) (Fig. 3A). Further we next examined the localization pattern of WASP or its PRR mutants in Jurkat T-cells conjugated to Raji B-cells pulsed with SEE toxin. In the conjugate in the presence of SEE pulsed Raji B-cells, WASP$_R$-RFP was localized at the T:B cell–cell contact site and it co-localized with actin. However, WASP mutant (WASP$_R^{S339Y}$-RFP) was not accumulated at the T:B contact site and it localized in the form of small patches inside the Jurkat T-cell (Fig. 3B). WASP$_R^{P373S}$-RFP or WASP$_R^{SP/YS}$-RFP was localized in a diffused pattern in T:B cell conjugates (Fig. 3B), thus suggesting that missense mutation in the PRR of WASP causing WAS affected the localization of WASP at the TCR activation site.

Fig. 1. Jurkat^{WKD} T-cells expressing WASP-PRR mutants were defective in chemotaxis towards SDF-1α. A) Western blot analysis of expression of endogenous WASP in Jurkat T-cells and Jurkat^{WKD} T-cells using anti-WASP antibody and anti-GAPDH (loading control). B) Average velocity of Jurkat^{WKD} T-cells expressing RFP, WASP$_R$-RFP, WASP$_R^{S339Y}$-RFP, WASP$_R^{P373S}$-RFP, and WASP$_R^{SP/YS}$-RFP. The velocity of sixty cells, 20 cells from each set from 3 independent experiments was used to calculate the mean. $^{**}P < 0.01$ compared to Jurkat^{WKD} T-cells expressing RFP (unpaired Student's *t*-test). C) Migration paths of 20 randomly chosen cells shown in the form of vector plot from Jurkat^{WKD} T-cells expressing RFP, WASP$_R$-RFP, WASP$_R^{S339Y}$-RFP, WASP$_R^{P373S}$-RFP, and WASP$_R^{SP/YS}$-RFP in Dunn chamber assay. Images were captured using time-lapse microscopy for 3.0 h at 2.0 min intervals. X and Y axis intersection points were taken as the starting point of each cell and the source of SDF-1α is at the top. D) Circular histogram representing the overall directionality of migration (final position of cells lie in 20° sector) towards the increasing concentration of chemokine (SDF-1α) source was plotted for 60 randomly chosen cells in Dunn chamber assay. E) Cell lysate of Jurkat^{WKD} cells expressing RFP, WASP$_R$-RFP, WASP$_R^{S339Y}$-RFP, WASP$_R^{P373S}$-RFP, and WASP$_R^{SP/YS}$-RFP was analyzed by Western blot using anti-WASP antibody and anti-GAPDH (loading control). F) Jurkat^{WKD} T-cells expressing (1) RFP, (2) WASP$_R$-RFP, (3) WASP$_R^{S339Y}$-RFP, (4) WASP$_R^{P373S}$-RFP, and (5) WASP$_R^{SP/YS}$-RFP were allowed to migrate for 3 h towards SDF-1α (100 ng/ml) containing media in the bottom well of a transwell. Percentage of cells migrated was calculated as the number of cells migrated to the bottom well to the initial cell number loaded to the upper well. The experiment was repeated thrice. $^{**}P < 0.01$ compared to Jurkat^{WKD} T-cells expressing RFP (unpaired Student's *t*-test).

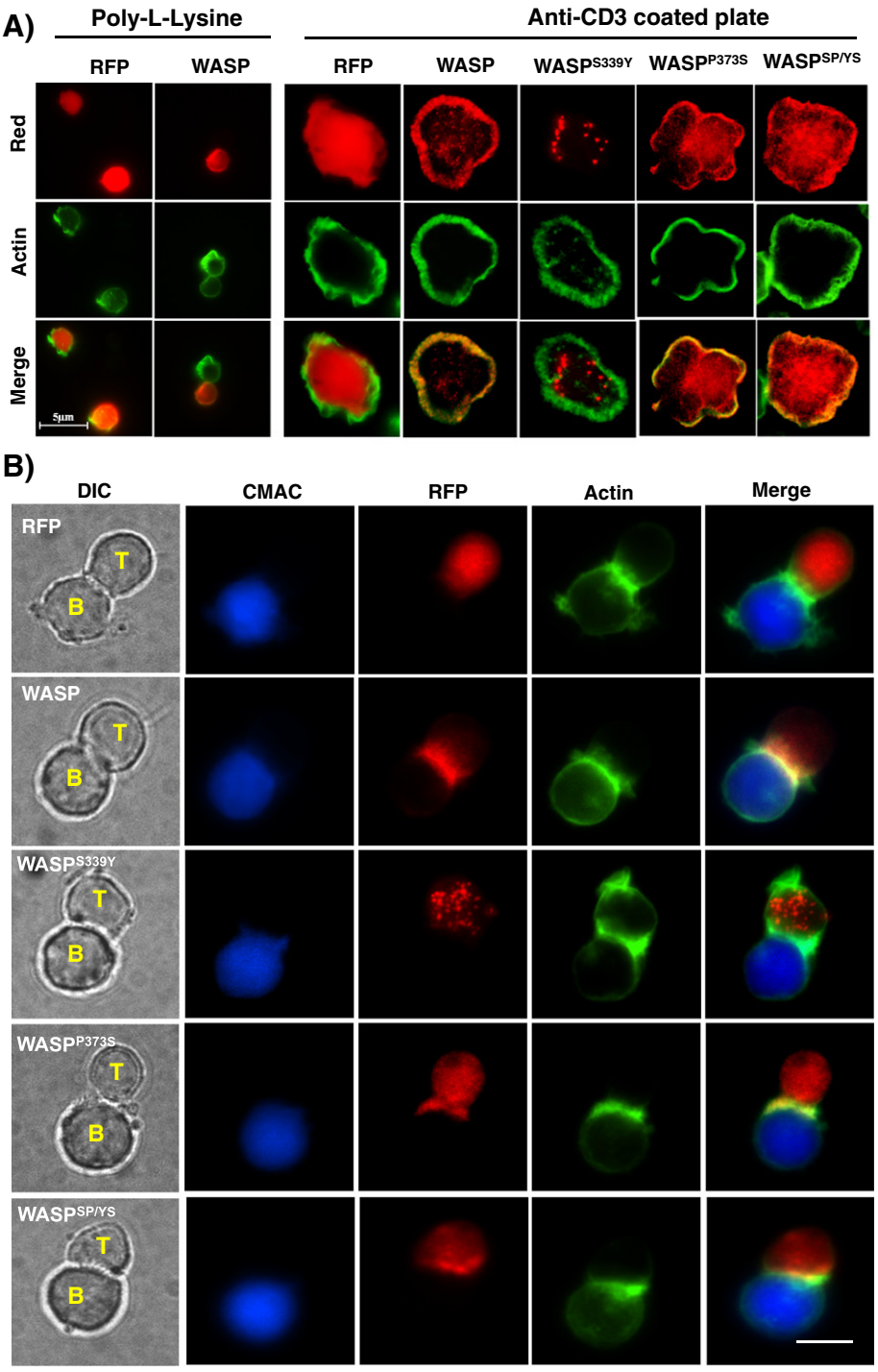

Fig. 3. WASP-PRR mutants have diffuse pattern of localization at TCR activation site and immunological synapse. A) Jurkat T-cells expressing RFP, $WASP_R$-RFP, $WASP_R^{S339Y}$-RFP, $WASP_R^{P373S}$-RFP, and $WASP_R^{SP/YS}$-RFP were plated on anti-CD3 (clone OKT3) antibody coated coverslip and poly-L-lysine coated plates. The cells were incubated at 37 °C for 5.0 min, fixed with 3.7% formaldehyde for 20 min and stained with Alexa 488 phalloidin. B) Jurkat T-cells expressing RFP, $WASP_R$-RFP, $WASP_R^{S339Y}$-RFP, $WASP_R^{P373S}$-RFP, and $WASP_R^{SP/YS}$-RFP were allowed to form conjugate with Raji B-cells pulsed with SEE toxin, plated on poly-L-lysine coated slides, fixed and stained with phalloidin 488 for F-actin staining. Bar = 5 μm.

3.4. Expression of $WASP_R^{P373S}$ or $WASP_R^{SP/YS}$ mutants does not rescue the IL-2 expression defect of Jurkat^{WKD} T-cells

T-cells from Wiskott–Aldrich Syndrome patients have defect in IL-2 production in response to TCR stimulation [31]. In order to determine whether WASP mutants ($WASP_R^{S339Y}$, $WASP_R^{P373S}$, $WASP_R^{SP/YS}$) regulate IL-2 gene transcription, Jurkat^{WKD} T-cells expressing $WASP_R$ or its mutants ($WASP_R^{S339Y}$, $WASP_R^{P373S}$ or $WASP_R^{SP/YS}$) or RFP alone (control) were plated on anti-CD3/anti-CD28 (2 μg/ml each) coated plate and incubated for 8 h. RNA from these cells was isolated and used for quantitative real-time PCR to check for IL-2 gene expression.

Expression of exogenous $WASP_R$ or $WASP_R^{S339Y}$ in Jurkat^{WKD} T-cells rescued the IL-2 gene transcription defect (behaved similar to Jurkat^{WT} T-cells, Fig. S1) while the expression of $WASP_R^{P373S}$ or $WASP_R^{SP/YS}$ mutants was unable to rescue the IL-2 gene transcription defect of Jurkat^{WKD} T-cells (behaved similar to Jurkat^{WKD} T-cells) (Fig. 4A). Impairment in IL-2 expression in $WASP_R^{P373S}$ or $WASP_R^{SP/YS}$ mutants expressing Jurkat^{WKD} T-cells was further confirmed by IL-2 ELISA

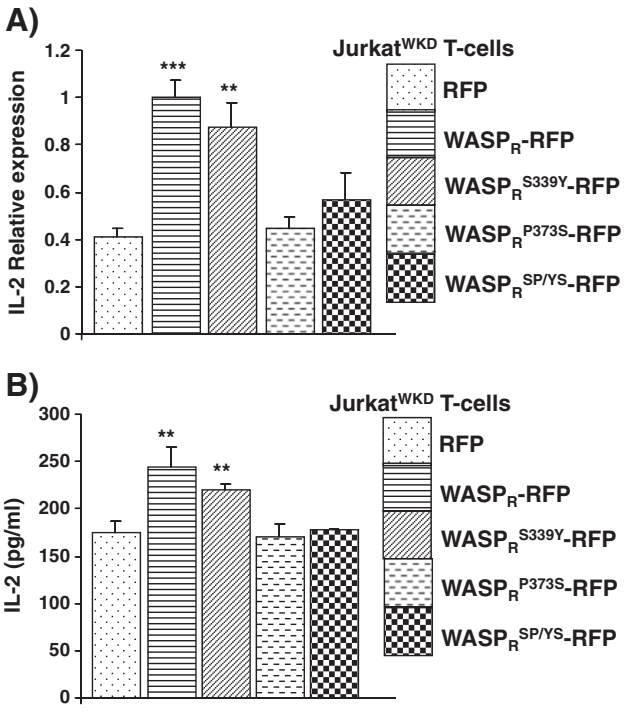

Fig. 4. WASP mutation, Pro373Ser abolished WASP mediated IL-2 gene expression. A) Jurkat^{WKD} T-cells expressing RFP, WASP$_R$-RFP, WASP$_R^{S339Y}$-RFP, WASP$_R^{P373S}$-RFP, and WASP$_R^{SP/YS}$-RFP were induced for 8 h on stimulatory surface (anti-CD3/anti-CD28 antibodies coated well; 2 μg/ml each). Total RNA was isolated, converted into cDNA and used to perform quantitative real time PCR for IL2 gene transcription. B) Cell culture supernatants from Jurkat^{WKD} T-cells expressing RFP, WASP$_R$-RFP, WASP$_R^{S339Y}$-RFP, WASP$_R^{P373S}$-RFP, and WASP$_R^{SP/YS}$-RFP (stimulated for 24 h with anti-CD3/CD28 along with cross-linking antibody) were collected and analyzed for IL-2 secretion by standard ELISA kit. $^{**}P < 0.01$; $^{***}P < 0.001$ compared to Jurkat^{WKD} T-cells expressing RFP (unpaired Student's *t*-test).

(Fig. 4B). The real time PCR data and IL-2 ELISA data shows that the point mutation (WASP^{P373S}) either alone or together with WASP^{S339Y} (WASP$^{SP/YS}$) did not rescue the IL-2 expression defect of Jurkat^{WKD} T-cells, suggesting that P373S mutation alone was sufficient for inhibiting WASP function in IL-2 expression. This result also suggests that the S339Y mutation in WASP does not impair WASP function in IL-2 expression in Jurkat T-cells.

3.5. WASP proline rich region mutations (S339Y or P373S) do not affect the interaction with known WASP binding proteins

The proline rich region of WASP has been shown to interact with a number of SH3 domain containing proteins (tyrosine kinases and adaptor proteins) which regulate WASP activation [17,32,33]. Tyrosine kinases activate WASP through tyrosine phosphorylation (Tyr^{291}) and destabilize WASP auto-inhibited conformation [34,35]. The two point mutations (Ser339Tyr and Pro373Ser) in the PRR of WASP may affect the interaction of WASP with SH3 domain containing proteins. In order to identify the effect of mutation on WASP–SH3 domain interaction a yeast two hybrid assay was performed using Gal4BD–WASP$_{1–503}$ (WT, WASP^{S339Y}, WASP^{P373S}, WASP$^{SP/YS}$) or Gal4BD–WASP$_{306–407}$ (WT, WASP^{S339Y}, WASP^{P373S}, WASP$^{SP/YS}$) as bait with Gal4AD–SH3 domain fusion constructs (Fyn, Fgr, Lyn, Hck, Src, Tec, Lck, Btk, PI3K, Abl, Nck1, Grb2, Toca-1, Irsp53, Cortactin, PSTPIP) was used as prey. The two WASP-PRR missense mutants individually (WASP^{S339Y} or WASP^{P373S}) or together (WASP$^{SY/PS}$) did not affect the interaction of WASP with SH3 domain containing proteins tested (data not shown). It is possible that there is more than one binding site for some of the SH3 domain containing proteins within the proline rich region of the WASP as well as in other regions of the WASP.

Expression of human WASP and WIP suppressed the growth defect of *las17Δ* strain; WASP–WIP interaction and a functional VCA domain on WASP are essential for suppression of growth defect of *las17Δ* strain [36]. In order to analyze the effect of WASP mutants (WASP^{S339Y}, WASP^{P373S}, WASP$^{SP/YS}$) on the formation of functional WIP–WASP complex, plasmids expressing WASP or its mutants were transformed into *las17Δ* cells together with either empty plasmid or plasmid expressing WIP. The transformants were streaked onto YPUAD agar plates and grown either at 24 °C or 37 °C for 3 days. The WASP-PRR mutants (WASP^{S339Y} or WASP^{P373S} or WASP$^{SP/YS}$) did not affect the ability of WASP to rescue the growth defect of *las17Δ* strain (Fig. 5A). Western blot analysis showed equal expression of WT WASP and its mutants in

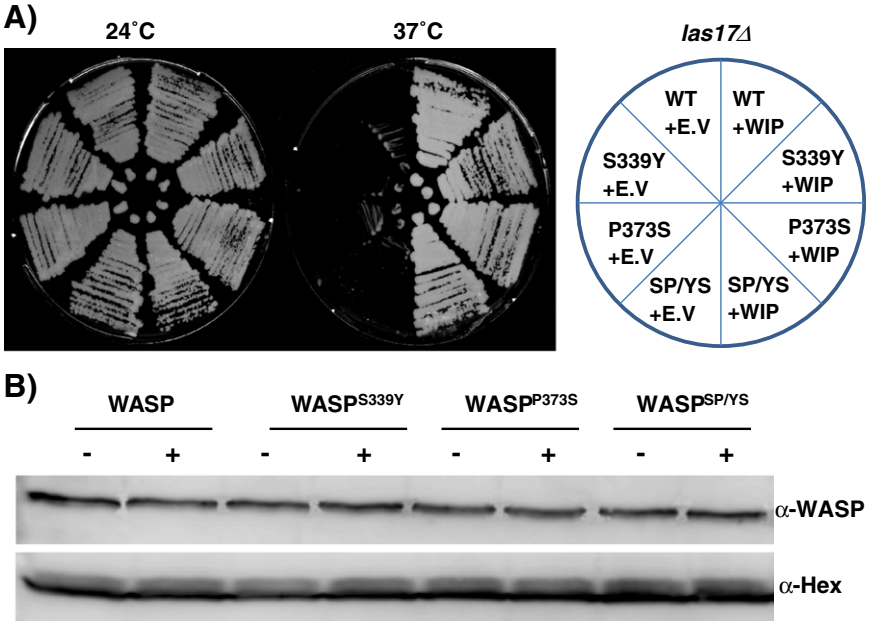

Fig. 5. WASP-PRR mutants suppressed the growth defects of *las17Δ* cells. A) *Las17Δ* yeast strain was transformed with plasmid expressing WASP (WT, WASP^{S339Y}, WASP^{P373S}, or WASP$^{SP/YS}$) with either empty vector or plasmid expressing WIP. The transformants were streaked on YPUAD agar plate and incubated at 24 °C and 37 °C after 3 days. B) The expression of WASP in the transformants in panel A was analyzed by Western blot using anti-WASP antibody and anti-Hexokinase antibody (loading control).

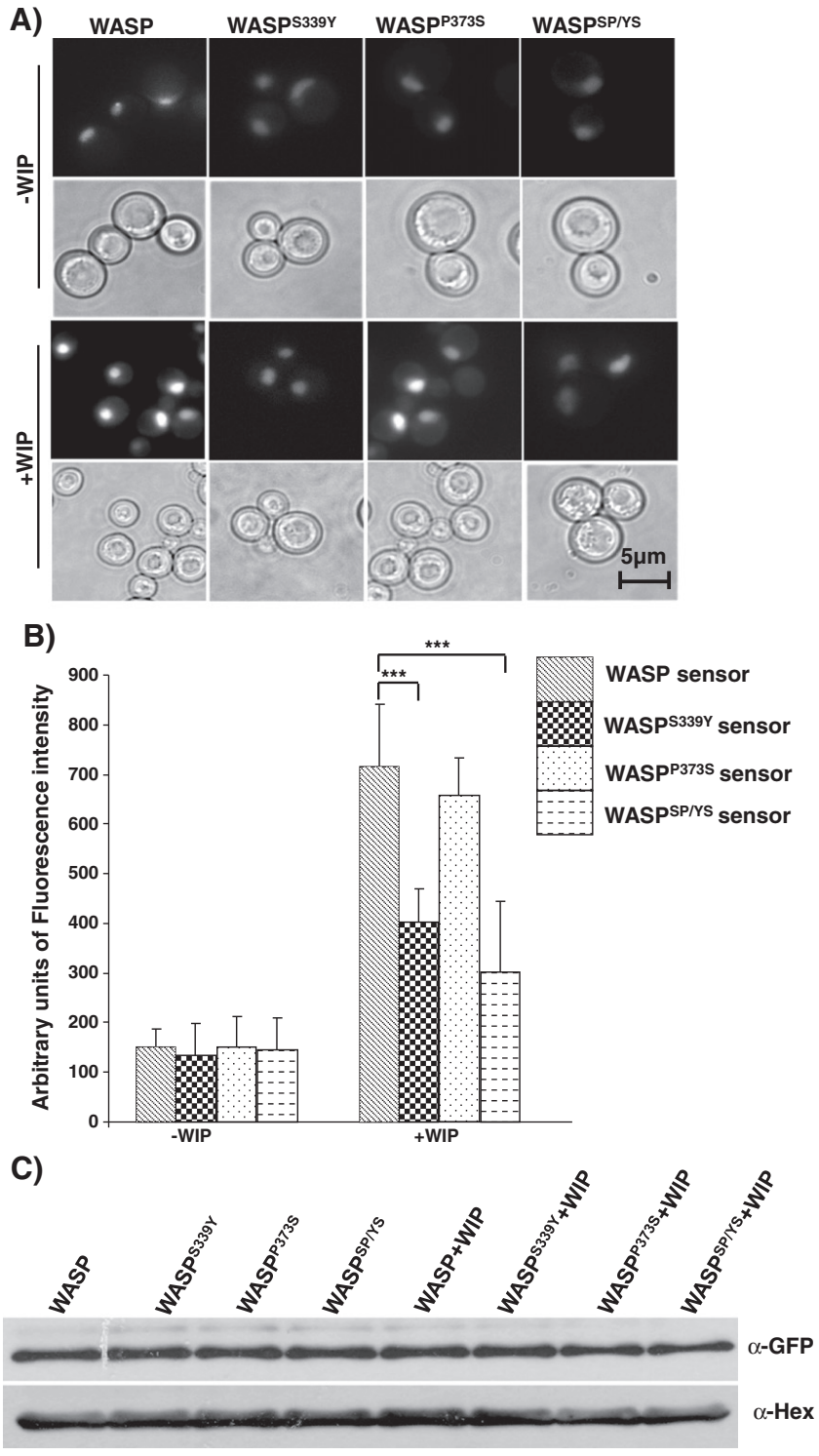

Fig. 6. WASP^{S339Y} mutation causes a partial open conformation. A) *S. cerevisiae* cells were transformed with WASP sensor (WT, WASP^{S339Y}, WASP^{P373S}, WASP$^{SP/YS}$) and either empty vector or plasmid expressing NLS–WIP. The transformants were grown at 24 °C in selective media and YFP signals in these cells were subsequently analyzed using fluorescence microscopy. Bar = 5 μm. B) Fluorescence signal quantification from 100 *S. cerevisiae* cells transformed with plasmids as described in panel A using MetaMorph software. $^{***}P < 0.001$ compared to WASP sensor + NLS–WIP (unpaired Student's *t*-test). C) Western blot analysis of expression of WASP in *S. cerevisiae* transformants (panel A) using anti-GFP antibody and anti-Hexokinase (loading control).

las17Δ cells (Fig. 5B). The results indicate that the mutations in the PRR do not affect the formation of functional WASP–WIP complex. Most importantly this result shows that the activity of both the N-terminus WH1 domain and the C-terminus VCA domain of WASP mutants is still functional.

3.6. WASP^{S339Y} and WASP$^{SP/YS}$ missense mutants adopt a partially open conformation in the presence of WIP

WASP exists in two different conformations, the auto-inhibited closed conformation which is stabilized by WIP and active open conformation

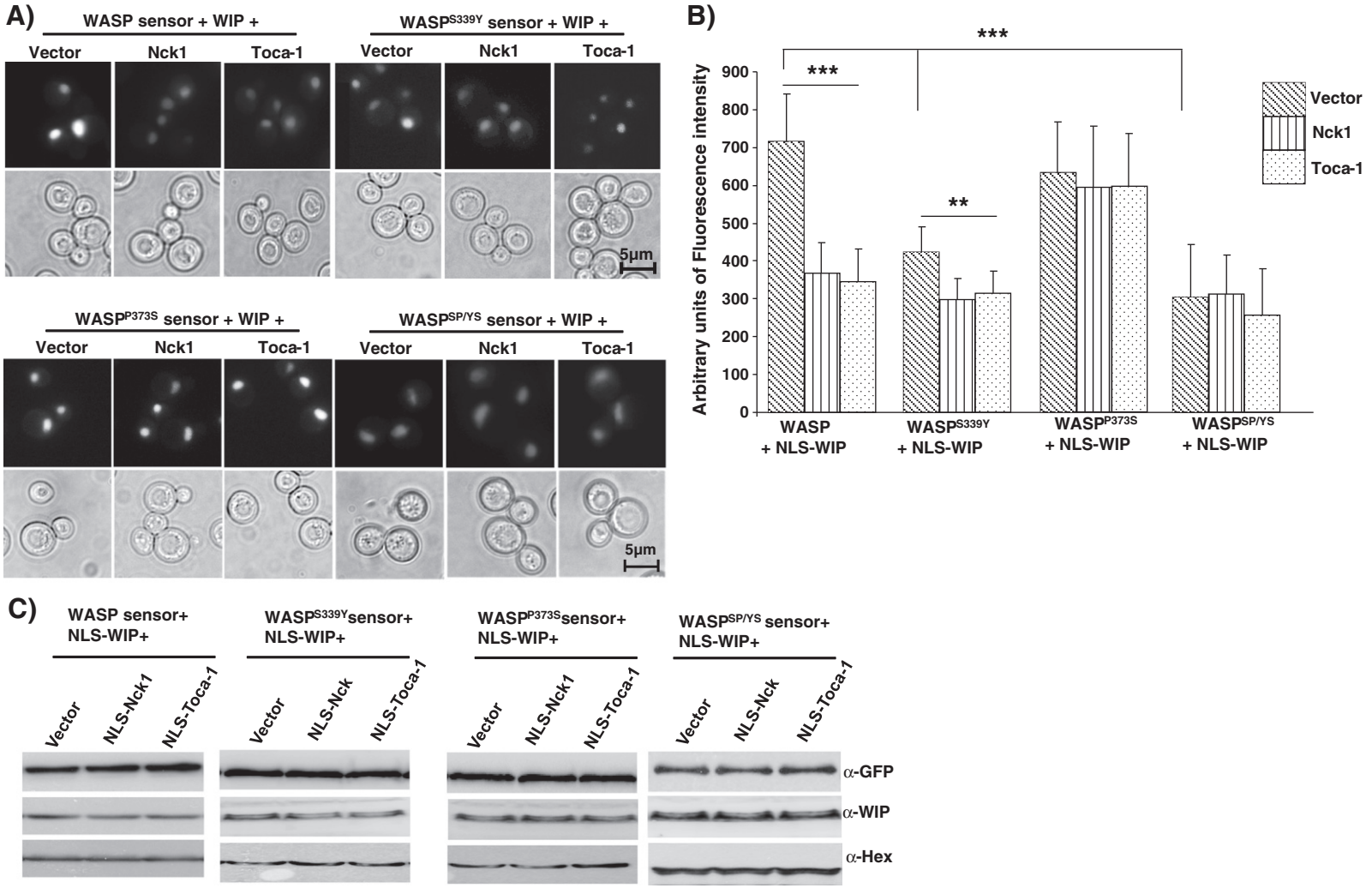

Fig. 7. Proline 373 is critical for Toca-1 and Nck1 mediated conformational changes of WASP. A) *S. cerevisiae* cells were transformed with three plasmids; 1) WASP sensor (WT, WASP^{S339Y} or WASP^{P373S} or WASP$^{SP/YS}$), 2) NLS–WIP, 3) empty vector, or plasmid expressing NLS–Nck1 or NLS–Toca1. The cells were grown at 24 °C in selective media and YFP signals in these cells were observed using fluorescence microscopy. Bar = 5 μm. B) Fluorescence signal quantification from 100 *S. cerevisiae* cells expressing genes as in panel A using MetaMorph software. $^{**}P < 0.01$; $^{***}P < 0.001$ (unpaired Student's *t*-test). C) Western blot analysis of expression of WASP (α-GFP) and WIP (α-WIP) in *S. cerevisiae* transformants (panel A). Anti-Hexokinase (α-Hex) antibody was used as loading control.

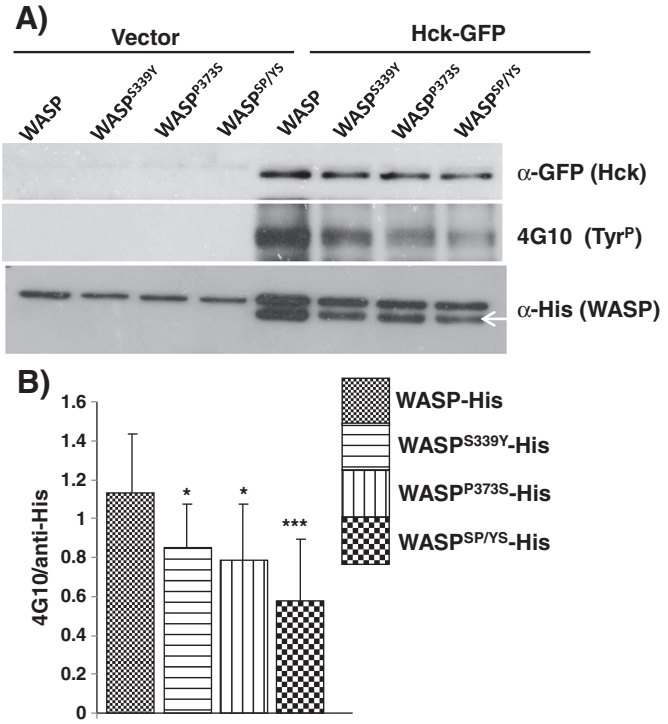

Fig. 8. $WASP^{SP/YS}$ mutant exhibits reduced phosphorylation by Hck. A) HEK293T cells were transfected with $WASP_R$-His (WT, $WASP_R^{S339Y}$, $WASP_R^{P373S}$, $WASP_R^{SP/YS}$) together with GFP or Hck-GFP. WASP or its mutants ($WASP_R^{S339Y}$, $WASP_R^{P373S}$, $WASP_R^{SP/YS}$) were isolated by His-tag pull-down assay. The proteins bound to the beads were analyzed by Western blot using anti-GFP (Hck), anti-His (WASP) antibody, and phospho-tyrosine using 4G10 antibody. Arrow head represents the degradation product of WASP or WASP-PRR mutants in the presence of Hck. B) Quantification of Western blots using densitometry. ImageJ software was used to perform densitometry analysis on three independent experiments. Band densities were measured as area under the curve. $^*P < 0.05$; $^{***}P < 0.001$ compared to WASP (unpaired Student's *t*-test).

[22,23]. WASP proline rich region missense mutants ($WASP^{S339Y}$, $WASP^{P373S}$ and $WASP^{SP/YS}$) do not affect interaction of WASP with SH3 domain containing proteins (data not shown) and formation of WASP–WIP complex; however the mutations might affect changes in the conformation of WASP. To analyze whether the missense mutations ($WASP^{S339Y}$ or $WASP^{P373S}$ or $WASP^{SP/YS}$) lead to changes in the conformation of $WASP^{S339Y}$ or $WASP^{P373S}$ or $WASP^{SP/YS}$, yeast strain PJ69-4A was transformed with WASP sensor (WT or $WASP^{S339Y}$ or $WASP^{P373S}$ or $WASP^{SP/YS}$) together with either NLS–WIP or empty vector. The construction of WASP or WASP-PRR mutant sensor was performed as described previously [23]. The transformants were grown to exponential phase at 24 °C and analyzed using fluorescence microscopy (Fig. 6A). The YFP fluorescence signals from 100 cells were quantified and plotted (Fig. 6B). The YFP fluorescence intensity of $WASP^{S339Y}$, $WASP^{P373S}$ and $WASP^{SP/YS}$ sensors was similar to WT WASP sensor in the absence of WIP. However the YFP fluorescence intensity of all the WASP sensors was enhanced significantly in the presence of WIP suggesting that WIP stabilizes the closed conformation of all the WASP sensors which is consistent with the previous findings [23].

The YFP fluorescence intensity of $WASP^{S339Y}$ sensor + WIP or $WASP^{SP/YS}$ sensor + WIP sensors but not $WASP^{P373S}$ sensor + WIP was significantly reduced compared to WASP sensor + WIP. However, the fluorescence intensity of $WASP^{SP/YS}$ sensor or $WASP^{S339Y}$ sensor was significantly increased in the presence of WIP compared to absence of WIP indicating that $WASP^{SP/YS}$ and $WASP^{S339Y}$ sensor exists in partially open conformation (Fig. 6A, B). The reduced fluorescence intensity of $WASP^{SP/YS}$ sensor could be the effect of $WASP^{S339Y}$ mutation alone as the YFP fluorescence intensity of $WASP^{P373S}$ sensor was similar to WASP sensor in the presence of WIP. Western blot analysis showed the similar expression of all WASP sensors either in the presence or in the absence of WIP indicating that the increase in fluorescence intensities of all the WASP sensors in the presence of WIP was not due to increased expression of sensor molecules (Fig. 6C). These results suggest that WASP-PRR point mutation (serine339 to tyrosine339 of WASP) S339Y, alters the WASP closed conformation in the presence of WIP.

3.7. Toca-1 and Nck1 further reduced the YFP fluorescence of $WASP^{S339Y}$ sensor in the presence of WIP

The single mutation $WASP^{S339Y}$ and the double mutant $WASP^{SP/YS}$ adopt a partial open conformation even in the presence of WIP (Fig. 6). Toca-1 and Nck1 have been shown to open up the closed conformation of WASP [23]. In order to analyze the effect of Toca-1 and Nck1 on conformational changes of $WASP^{S339Y}$, yeast cells expressing WASP sensor/NLS–WIP or $WASP^{S339Y}$ sensor/NLS–WIP were transformed with empty vector or plasmids expressing NLS–Toca-1 or NLS–Nck1. The transformants were then analyzed using fluorescence microscopy (Fig. 7A).

Analysis of fluorescence intensity (Fig. 7B) revealed that both Toca-1 and Nck1 further reduced the YFP fluorescence from $WASP^{S339Y}$ sensor. The Western blot analysis of $WASP^{S339Y}$ sensor showed its similar expression in all the respective transformants (Fig. 7C). These results indicate that Toca-1 or Nck1 induces conformational changes of $WASP^{S339Y}$ sensor suggesting formation of a functional $WASP^{S339Y}$–Toca-1 or $WASP^{S339Y}$–Nck1 complex.

3.8. Toca-1 or Nck1 does not relieve the auto-inhibition of $WASP^{P373S}$ sensor

WASP and N-WASP are multi-domain proteins which have been shown to be regulated by a number of other interacting proteins. Yeast two hybrid assay (data not shown) suggested that $WASP^{P373S}$ and $WASP^{SP/YS}$ interact with both Toca-1 and Nck1; however it might affect the formation of functional WASP–Toca-1 or WASP–Nck1 complex. Result from previous section revealed that $WASP^{P373S}$ exists in closed conformation in the presence of WIP similar to WASP (Fig. 6).

In order to analyze the effect of Toca-1 or Nck1 on conformation changes, yeast cells expressing $WASP^{P373S}$ sensor and NLS–WIP were transformed with empty vector or plasmid expressing NLS–Toca-1 or NLS–Nck1. The transformants were analyzed using fluorescence microscopy (Fig. 7A). Analysis of fluorescence intensity (Fig. 7B) revealed that both Toca-1 and Nck1 did not cause a decrease in the fluorescence intensity of $WASP^{P373S}$ sensor. However, both Toca1 and Nck1 reduced the fluorescence intensity of WT WASP sensor (Fig. 7). Western blot analysis showed the similar expression of $WASP^{P373S}$ sensor in all respective co-transformants (Fig. 7C). Taken together these results indicate that both Toca-1 and Nck1 can disrupt the auto-inhibitory loop of WASP even in the presence of WIP which is consistent with previous report [23] but fail to relieve the auto-inhibition of $WASP^{P373S}$ mutant. Toca-1 or Nck1 had no effect on $WASP^{SP/YS}$ sensor suggesting that the mutation (P373S) may be inhibiting further changes in conformation of $WASP^{SP/YS}$ sensor by Toca1 or Nck1.

3.9. WASP-PRR mutations decreased the Hck mediated WASP tyrosine phosphorylation

The SH3 domain of Hck (tyrosine kinase) has been shown to interact with WASP at the proline rich region resulting in WASP-Tyr^{291} phosphorylation and WASP activation [34]. Therefore, the effect of WASP-PRR mutants on Hck mediated tyrosine phosphorylation of WASP was analyzed. HEK293T cells were transfected with WASP-His or WASP-PRR mutants ($WASP^{S339Y}$ or $WASP^{P373S}$ or $WASP^{SP/YS}$) tagged with His-tag together with empty vector or plasmid expressing Hck-GFP. The cells were lysed 36 h after transfections and His-tag pull-down assay was performed. The tyrosine-phosphorylation levels of WASP or WASP-PRR mutants were detected using phosphotyrosine specific

antibody, 4G10. Western blot analysis revealed that WASP-PRR mutants still bound to Hck (Fig. 8) which is consistent with yeast two hybrid assay (data not shown). Quantification of Western blots using densitometry analysis revealed that WASP-PRR mutants had significantly reduced Hck mediated tyrosine phosphorylation (Fig. 8). No WASP tyrosine phosphorylation was detected when the cells were transfected with WASP or WASP-PRR mutants without Hck indicating that the phosphorylation levels detected in the Western blots were due to exogenous Hck expression. Thus, these results indicate that WASP-PRR mutations either individual or together decreased the Hck mediated WASP tyrosine phosphorylation.

4. Discussion

Wiskott–Aldrich Syndrome is caused by mutations in the gene encoding WASP, an adaptor protein which regulates the actin cytoskeleton by activating the Arp2/3 complex [3]. Majority of the WASP missense mutations are found in the WH1 domain of WASP [16,17]; which mediates interaction with WIP [6]. We have previously shown that mutations located outside the WH1 domain of WASP do not affect the activity of WASP in *S. cerevisiae las17Δ* strain [19]. Two missense mutations (S339Y, P373S) in the PRR of WASP have been reported to occur together in WAS patients; however the molecular defect caused by these mutations or the contribution of each mutation to the clinical outcome has not been characterized.

WASP knockdown Jurkat T-cells ($Jurkat^{WKD}$ T-cells) are defective in chemotaxis towards SDF-1 , had reduced migration velocity and are defective in IL2 expression upon activation similar to T-cells from WAS patients [31]. $Jurkat^{WKD}$ T-cells expressing WASP-PRR mutants ($WASP_R^{S339Y}$, $WASP_R^{P373S}$, $WASP_R^{SP/YS}$) had migration velocities comparable to cells expressing $WASP_R$ (Fig. 1B). However the mutants were not able to rescue the chemotaxis defect of $Jurkat^{WKD}$ T-cells in both Dunn chamber and transwell chemotaxis assay (Fig. 1). Actin cytoskeleton rearrangement to form membrane projections upon stimulation with anti-CD3/anti-CD28 was also defective in $Jurkat^{WKD}$ T-cell expressing WASP-PRR mutants compared to $Jurkat^{WKD}$ T-cells expressing $WASP_R$ (Fig. 2). Thus both the mutations either individually or together affect the chemotaxis and actin cytoskeleton remodeling in T-cells. However the mutations either individually or together did not affect the conformation, stability or activity of the WH1 domain and VCA domain of WASP in regulating the actin cytoskeleton of *S. cerevisiae* as all the mutants suppressed the growth defect of *las17*Δ cells together with WIP (Fig. 5).

WASP is critical for T-cell activation and IL2 expression upon TCR stimulation [31]. The PRR of WASP is critical for its localization to T-cell:APC contact site [25]. Though WASP-PRR mutations did not affect the interaction of WASP with Nck1 (data not shown), the localization of WASP-PRR mutants was disrupted (Fig. 3). $WASP_R^{S339Y}$-RFP localized in the form of small clusters compared to the co-localization of $WASP_R$-RFP with actin at the cell periphery and T-cell:B cell contact site. Expression of $WASP_R^{S339Y}$ rescued the IL-2 expression defect of $Jurkat^{WKD}$ T-cell (Fig. 4) indicating that $WASP_R^{S339Y}$ mutant can form functional contacts with downstream effectors required for T-cell activation. The localization of $WASP_R^{P373S}$-RFP was diffused throughout the spread cell with some co-localization with actin at the cell periphery (Fig. 3) and this mutant was unable to rescue the IL-2 gene transcription defect of $Jurkat^{WKD}$ T-cells. $WASP_R^{SP/YS}$-RFP behaved similar to $WASP_R^{P373S}$-RFP in terms of its localization pattern at TCR contact sites and T-cell activation, suggesting a dominant effect of $WASP^{P373S}$ mutation over the $WASP^{S339Y}$ mutation (Figs. 3, 4). $WASP^{S339Y}$ mutant was unable to rescue the chemotaxis but it can rescue the IL-2 gene transcription defect of $Jurkat^{WKD}$ T-cell. This is consistent with earlier reports that the activity of WASP in regulating actin cytoskeleton is independent of its role in IL2 transcription [37]. Thus our results suggest that Pro373Ser mutation abolishes all the activities of WASP in T-cells while Ser339Tyr abolishes only the actin cytoskeleton regulatory activities of WASP.

WASP has been shown to adopt intra-molecular closed conformation mediated by interaction between GBD and VCA regions of WASP [22]. This auto-inhibitory closed conformation of WASP has been suggested to be stabilized by interaction with WIP [23,38]. The proline rich region of WASP has been shown to interact with SH3 domain containing proteins [17], and binding of Toca-1 or Nck1 can relieve this auto-inhibitory conformation [23]. The mutations ($WASP^{S339Y}$ or $WASP^{P373S}$ or $WASP^{SP/YS}$) did not affect the interaction with sixteen known WASP binding proteins including Toca-1 and Nck1 (data not shown). It is possible that there is more than one binding site on WASP for some of these proteins and the point mutations may have affected only one of these binding sites. For instance, the Src kinase Fyn has been shown to interact with the PRR of WASP [39] and $WASP_{1-170}$ [40]. All these results suggest that WASP is likely to have more than one binding sites for interaction with SH3 domain containing proteins. The conformational analysis of WASP and its mutants using BiFC assay as described previously [23] revealed that $WASP^{S339Y}$ and $WASP^{SP/YS}$ sensors adopt partially open conformation compared to WASP and $WASP^{P373S}$ sensors in the presence of WIP. However, unlike WASP, the closed conformation of $WASP^{P373S}$ sensor was not altered in the presence of either Toca-1 or Nck1 (Fig. 7) suggesting that Pro373 is crucial for conformational change of WASP. In contrast to $WASP^{P373S}$ sensor, the fluorescence intensity of $WASP^{S339Y}$ was reduced in the presence of either Toca-1 or Nck1 (Fig. 7). The fluorescence intensity of $WASP^{SP/YS}$ sensor was not reduced in the presence of Toca1 or Nck1 probably due to the presence of Pro373Ser mutation which does not allow changes in the conformation of WASP. The altered conformation of WASP-PRR mutants was neither due to any loss of interaction of WASP mutants with SH3 domain containing proteins (data not shown) nor due to loss of interaction with active Cdc42 molecule (Fig. S2). Thus, the altered conformation of $WASP^{P373S}$ or $WASP^{SP/YS}$ mutants may not be responsible for loss of WASP interaction with upstream activators (SH3 domain containing protein; data not shown) but it could be responsible for defects in activation of WASP downstream effectors essential for IL-2 production. The altered conformation of WASP-PRR mutants might affect the WASP phosphorylation as WASP mutant L270P unfolded the WASP molecule and had increased the basal level of WASP phosphorylation [35]. Phosphorylation of WASP-PRR mutants was not affected in Jurkat T-cell when stimulated with anti-CD3/C28 antibodies (Fig. S3). However, these mutations caused significant reduction in Hck mediated tyrosine phosphorylation of WASP in HEK293T cells (Fig. 8). This difference could be due to the presence of other WASP regulator in Jurkat T-cells such as Fyn which regulates the WASP phosphorylation upon TCR stimulation [41] as well as increased turnover of WT WASP upon phosphorylation [42]. $Tyorsine^{291}$ phosphorylation of WASP has been shown to destabilize the auto-inhibitory loop formed between the basic region and VCA domain of WASP and facilitated the binding of Arp2/3 complex and actin polymerization [34,43]. Phosphorylation of WASP has been shown to be important for WASP turnover and cell migration as inhibition of WASP turnover by inhibiting calpain impaired dendritic cell motility [44]. Hck has been shown to phosphorylate WASP upon chemo-attractant stimuli [45]. Hck mediated tyrosine phosphorylation of WASP-PRR mutations was reduced compared to WT WASP (Fig. 8) indicating critical effect of both the WASP mutations on Jurkat T-cell motility, thus, causing defective homing of T-cells and being responsible for WAS. Expression of WASP confers a selective advantage for T-cells [46] and a number of reports have shown that patients with mutations which cause severe WAS exhibit revertant mosaicism where a second-site mutation leads to altered but functional gene products [47,48].

We have shown that though WAS patients had two mutations together, $WASP^{P373S}$ mutation alone compromised all activity of WASP in T-cells. Proline 373 of WASP is crucial for relieving WASP from the closed conformation and Pro373Ser mutation abolished the conformational changes required for the activity of WASP in promoting IL2 expression and chemotaxis. $WASP^{S339Y}$ mutation compromised only the

actin cytoskeleton's regulatory role of WASP without affecting WASP role in IL2 transcription and the $WASP^{S339Y}$ mutant adopted a partial opened conformation. This mutation in the double mutants allowed $WASP^{SP/YS}$ to adopt a partial open conformation and probably reduces the severity of the clinical symptoms.

Acknowledgements

This work was supported by grants from the Academic Research Fund Tier 1 (MOE) RG28/05 and RG52/10. We declare that there is no conflict of interest.

Appendix A. Supplementary data

Supplementary data to this article can be found online at http://dx.doi.org/10.1016/j.bbadis.2014.01.006.

References

[1] A. Wiskott, *Familiärer, angeborener Morbus Werlhofii?* Mon. J.Pediatr. 68 (1937) 212–216.
[2] R.A. Aldrich, A.G. Steinberg, D.C. Campbell, Pedigree demonstrating a sex-linked recessive condition characterized by draining ears, eczematoid dermatitis and bloody diarrhea, Pediatrics 13 (1954) 133–139.
[3] J.M. Derry, H.D. Ochs, U. Francke, Isolation of a novel gene mutated in Wiskott–Aldrich syndrome, Cell 78 (1994) 635–644.
[4] J.M. Derry, J.A. Kerns, K.I. Weinberg, H.D. Ochs, V. Volpini, X. Estivill, A.P. Walker, U. Francke, WASP gene mutations in Wiskott–Aldrich syndrome and X-linked thrombocytopenia, Hum. Mol. Genet. 4 (1995) 1127–1135.
[5] K. Devriendt, A.S. Kim, G. Mathijs, S.G. Frints, M. Schwartz, J.J. Van Den Oord, G.E. Verhoef, M.A. Boogaerts, J.P. Fryns, D. You, M.K. Rosen, P. Vandenberghe, Constitutively activating mutation in WASP causes X-linked severe congenital neutropenia, Nat. Genet. 27 (2001) 313–317.
[6] N. Ramesh, I.M. Anton, J.H. Hartwig, R.S. Geha, WIP, a protein associated with Wiskott–Aldrich syndrome protein, induces actin polymerization and redistribution in lymphoid cells, Proc. Natl. Acad. Sci. U. S. A. 94 (1997) 14671–14676.
[7] T. Wada, G.J. Jagadeesh, D.L. Nelson, F. Candotti, Retrovirus-mediated WASP gene transfer corrects Wiskott–Aldrich syndrome T-cell dysfunction, Hum. Gene Ther. 13 (2002) 1039–1046.
[8] M.D. Gallego, M.A. de la Fuente, I.M. Anton, S. Snapper, R. Fuhlbrigge, R.S. Geha, WIP and WASP play complementary roles in T cell homing and chemotaxis to SDF-1alpha, Int. Immunol. 18 (2006) 221–232.
[9] D. Kenney, L. Cairns, E. Remold-O'Donnell, J. Peterson, F.S. Rosen, R. Parkman, Morphological abnormalities in the lymphocytes of patients with the Wiskott–Aldrich syndrome, Blood 68 (1986) 1329–1332.
[10] S.B. Snapper, F.S. Rosen, E. Mizoguchi, P. Cohen, W. Khan, C.H. Liu, T.L. Hagemann, S.P. Kwan, R. Ferrini, L. Davidson, A.K. Bhan, F.W. Alt, Wiskott–Aldrich syndrome protein-deficient mice reveal a role for WASP in T but not B cell activation, Immunity 9 (1998) 81–91.
[11] J. Zhang, A. Shehabeldin, L.A. da Cruz, J. Butler, A.K. Somani, M. McGavin, I. Kozieradzki, A.O. dos Santos, A. Nagy, S. Grinstein, J.M. Penninger, K.A. Siminovitch, Antigen receptor-induced activation and cytoskeletal rearrangement are impaired in Wiskott–Aldrich syndrome protein-deficient lymphocytes, J. Exp. Med. 190 (1999) 1329–1342.
[12] S.B. Snapper, F.S. Rosen, The Wiskott–Aldrich Syndrome Protein (WASP): roles in signaling and cytoskeletal organization, Annu. Rev. Immunol. 17 (1999) 905–929.
[13] T. Takenawa, S. Suetsugu, The WASP–WAVE protein network: connecting the membrane to the cytoskeleton, Nat. Rev. Mol. Cell Biol. 8 (2007) 37–48.
[14] P. Aspenstrom, The verprolin family of proteins: regulators of cell morphogenesis and endocytosis, FEBS Lett. 579 (2005) 5253–5259.
[15] R.C. Robinson, K. Turbedsky, D.A. Kaiser, J.B. Marchand, H.N. Higgs, S. Choe, T.D. Pollard, Crystal structure of Arp2/3 complex, Science 294 (2001) 1679–1684.
[16] Y. Jin, C. Mazza, J.R. Christie, S. Giliani, M. Fiorini, P. Mella, F. Gandellini, D.M. Stewart, Q. Zhu, D.L. Nelson, L.D. Notarangelo, H.D. Ochs, Mutations of the Wiskott–Aldrich Syndrome Protein (WASP): hotspots, effect on transcription, and translation and phenotype/genotype correlation, Blood 104 (2004) 4010–4019.
[17] K. Imai, S. Nonoyama, H.D. Ochs, WASP (Wiskott–Aldrich Syndrome Protein) gene mutations and phenotype, Curr. Opin. Allergy Clin. Immunol. 3 (2003) 427–436.
[18] D.M. Stewart, L. Tian, D.L. Nelson, Mutations that cause the Wiskott–Aldrich syndrome impair the interaction of Wiskott–Aldrich Syndrome Protein (WASP) with WASP interacting protein, J. Immunol. 162 (1999) 5019–5024.
[19] R. Rajmohan, A. Raodah, M.H. Wong, T. Thanabalu, Characterization of Wiskott–Aldrich syndrome (WAS) mutants using *Saccharomyces cerevisiae*, FEMS Yeast Res. 9 (2009) 1226–1235.
[20] M.A. de la Fuente, Y. Sasahara, M. Calamito, I.M. Antón, A. Elkhal, M.D. Gallego, K. Suresh, K. Siminovitch, H.D. Ochs, K.C. Anderson, F.S. Rosen, R.S. Geha, N. Ramesh, WIP is a chaperone for Wiskott–Aldrich syndrome protein (WASP), Proc. Natl. Acad. Sci. 104 (2007) 926–931.
[21] K. Schwarz, WASPbase: a database of WAS- and XLT-causing mutations, Immunol. Today 17 (1996) 496–502.
[22] A.S. Kim, L.T. Kakalis, N. Abdul-Manan, G.A. Liu, M.K. Rosen, Autoinhibition and activation mechanisms of the Wiskott–Aldrich syndrome protein, Nature 404 (2000) 151–158.
[23] R.P. Lim, A. Misra, Z. Wu, T. Thanabalu, Analysis of conformational changes in WASP using a split YFP, Biochem. Biophys. Res. Commun. 362 (2007) 1085–1089.
[24] K. Badour, J. Zhang, F. Shi, M.K. McGavin, V. Rampersad, L.A. Hardy, D. Field, K.A. Siminovitch, The Wiskott–Aldrich syndrome protein acts downstream of CD2 and the CD2AP and PSTPIP1 adaptors to promote formation of the immunological synapse, Immunity 18 (2003) 141–154.
[25] J.L. Cannon, C.M. Labno, G. Bosco, A. Seth, M.H. McGavin, K.A. Siminovitch, M.K. Rosen, J.K. Burkhardt, WASP recruitment to the T cell:APC contact site occurs independently of Cdc42 activation, Immunity 15 (2001) 249–259.
[26] S.N. Naqvi, R. Zahn, D.A. Mitchell, B.J. Stevenson, A.L. Munn, The WASp homologue Las17p functions with the WIP homologue End5p/verprolin and is essential for endocytosis in yeast, Curr. Biol. 8 (1998) 959–962.
[27] D. Zicha, G. Dunn, G. Jones, Analyzing chemotaxis using the Dunn direct-viewing chamber, Methods Mol. Biol. 75 (1997) 449–457.
[28] M. Barda-Saad, A. Braiman, R. Titerence, S.C. Bunnell, V.A. Barr, L.E. Samelson, Dynamic molecular interactions linking the T cell antigen receptor to the actin cytoskeleton, Nat. Immunol. 6 (2005) 80–89.
[29] I.J. Molina, D.M. Kenney, F.S. Rosen, E. Remold-O'Donnell, T cell lines characterize events in the pathogenesis of the Wiskott–Aldrich syndrome, J. Exp. Med. 176 (1992) 867–874.
[30] N. Andreu, J.M. Aran, C. Fillat, Novel membrane cell projection defects in Wiskott–Aldrich syndrome B cells, Int. J. Mol. Med. 20 (2007) 445–450.
[31] R. Badolato, S. Sozzani, F. Malacarne, S. Bresciani, M. Fiorini, A. Borsatti, A. Albertini, A. Mantovani, A.G. Ugazio, L.D. Notarangelo, Monocytes from Wiskott–Aldrich patients display reduced chemotaxis and lack of cell polarization in response to monocyte chemoattractant protein-1 and formyl-methionyl-leucyl-phenylalanine, J. Immunol. 161 (1998) 1026–1033.
[32] A. Dovas, D. Cox, Regulation of WASp by phosphorylation: activation or other functions? Commun. Integr. Biol. 3 (2010) 101–105.
[33] A.J. Thrasher, S.O. Burns, WASP: a key immunological multitasker, Nat. Rev. Immunol. 10 (2010) 182–192.
[34] G.O. Cory, R. Garg, R. Cramer, A.J. Ridley, Phosphorylation of tyrosine 291 enhances the ability of WASp to stimulate actin polymerization and filopodium formation. Wiskott–Aldrich syndrome protein, J. Biol. Chem. 277 (2002) 45115–45121.
[35] H. Park, D. Cox, Cdc42 regulates Fc gamma receptor-mediated phagocytosis through the activation and phosphorylation of Wiskott–Aldrich syndrome protein (WASP) and neural-WASP, Mol. Biol. Cell 20 (2009) 4500–4508.
[36] R. Rajmohan, L. Meng, S. Yu, T. Thanabalu, WASP suppresses the growth defect of *Saccharomyces cerevisiae* las17Delta strain in the presence of WIP, Biochem. Biophys. Res. Commun. 342 (2006) 529–536.
[37] C. Silvin, B. Belisle, A. Abo, A role for Wiskott–Aldrich syndrome protein in T-cell receptor-mediated transcriptional activation independent of actin polymerization, J. Biol. Chem. 276 (2001) 21450–21457.
[38] N. Martinez-Quiles, R. Rohatgi, I.M. Anton, M. Medina, S.P. Saville, H. Miki, H. Yamaguchi, T. Takenawa, J.H. Hartwig, R.S. Geha, N. Ramesh, WIP regulates N-WASP-mediated actin polymerization and filopodium formation, Nat. Cell Biol. 3 (2001) 484–491.
[39] S. Banin, O. Truong, D.R. Katz, M.D. Waterfield, P.M. Brickell, I. Gout, Wiskott–Aldrich syndrome protein (WASP) is a binding partner for c-Src family protein-tyrosine kinases, Curr. Biol. 6 (1996) 981–988.
[40] M. Sato, R. Sawahata, T. Takenouchi, H. Kitani, Identification of Fyn as the binding partner for the WASP N-terminal domain in T cells, Int. Immunol. 23 (2011) 493–502.
[41] K. Badour, J. Zhang, K.A. Siminovitch, Involvement of the Wiskott–Aldrich syndrome protein and other actin regulatory adaptors in T cell activation, Semin. Immunol. 16 (2004) 395–407.
[42] B. Reicher, N. Joseph, A. David, M.H. Pauker, O. Perl, M. Barda-Saad, Ubiquitylation-dependent negative regulation of WASp is essential for actin cytoskeleton dynamics, Mol. Cell. Biol. 32 (2012) 3153–3163.
[43] E. Torres, M.K. Rosen, Contingent phosphorylation/dephosphorylation provides a mechanism of molecular memory in WASP, Mol. Cell 11 (2003) 1215–1227.
[44] Y. Calle, N.O. Carragher, A.J. Thrasher, G.E. Jones, Inhibition of calpain stabilises podosomes and impairs dendritic cell motility, J. Cell Sci. 119 (2006) 2375–2385.
[45] Y. Shi, B. Dong, H. Miliotis, J. Liu, A.S. Alberts, J. Zhang, K.A. Siminovitch, Src kinase Hck association with the WASp and mDia1 cytoskeletal regulators promotes chemoattractant-induced Hck membrane targeting and activation in neutrophils, Biochem. Cell Biol. 87 (2009) 207–216.
[46] K. Boztug, M. Germeshausen, I. Avedillo Diez, V. Gulacsy, J. Diestelhorst, M. Ballmaier, K. Welte, L. Marodi, L. Chernyshova, C. Klein, Multiple independent second-site mutations in two siblings with somatic mosaicism for Wiskott–Aldrich syndrome, Clin. Genet. 74 (2008) 68–74.
[47] T. Wada, A. Konno, S.H. Schurman, E.K. Garabedian, S.M. Anderson, M. Kirby, D.L. Nelson, F. Candotti, Second-site mutation in the Wiskott–Aldrich syndrome (WAS) protein gene causes somatic mosaicism in two WAS siblings, Eur. J. Clin. Invest. 111 (2003) 1389–1397.
[48] W. Du, S. Kumaki, T. Uchiyama, A. Yachie, C. Yeng Looi, S. Kawai, M. Minegishi, N. Ramesh, R.S. Geha, Y. Sasahara, S. Tsuchiya, A second-site mutation in the initiation codon of WAS (WASP) results in expansion of subsets of lymphocytes in an Wiskott–Aldrich syndrome patient, Hum. Mutat. 27 (2006) 370–375.